ISSN 1392 - 1207. MECHANIKA. 2011. 17(2): 156-161

Numerical study on hydraulic and thermal characteristics of a minichannel heat sink with impinging air flow

M. Beriache*, A. Bettahar*, L. Loukarfi*, L. Mokhtar Saïdia*, H. Naji**

**Université Hassiba Benbouali, BP 151, Hay Essalem, Chlef (02000), Algeria, E-mail: m.beriache@gmail.com*

***Laboratoire Génie Civil et géo-Environnement (LGCgE- EA 4515), Université d'Artois/FSA Béthune, Université Lille Nord de France, F-59000 Lille, France, F-62400 Béthune, France, E-mail: hassane.naji@univ-artois.fr*

crossref http://dx.doi.org/10.5755/j01.mech.17.2.331

Nomenclature

A - heat transfer area, m²; C_P - specific heat coefficient, J/kg K; D_h - hydraulic diameter, m; h - convective heat transfer coefficient, w/m²K; h_b - height of the base, m; H - height of a minichannel fin, m; λ - thermal conductivity of a aluminium, W/m K; L - length of the base of a minichannel heat sink, m; l_c - channel width, m; L^* - dimensionless thermal developing flow length; $\dot{m}$ - mass flow rate, kg/s; N_f - number of fins; n - number of channels; Nu - Nusselt number; p - pressure, Pa; Q - power of heat source, W; q'' - heat flux, W/m²; R_e - Reynolds number; R_{th} - thermal resistance, °C/W; t_f - fin thickness, m; T - temperature, °C; u - velocity in the x-direction, m/s; V - velocity in the y-direction, m/s; V_0 - inlet velocity, m/s; $\dot{V}$ - air flow rate, m³/s; W - width of the base, m; w_C - channel width, m; ρ - air density, kg/m³; μ - dynamic viscosity, Ns/m²; x, y, z-space variables.

1. Introduction

As electronic equipment becomes smaller and more advanced, it necessitates higher circuit integration per unit area, which in turn contributes to a rapid increase of heat generation [1].

Thus, the effective removal of heat dissipations and the maintaining the chip at a safe operating temperature have played an important role in ensuring a reliable operation of electronic components [1]. There are many methods in electronics cooling, such as jet impingement cooling and heat pipe [2]. Conventional cooling electronics normally used impinging jet with heat sink showing superiority in terms of unit price, weight and reliability. Therefore, the most common way to enhance the air-cooling is through the utilization of impingement air jet on a mini or microchannel heat sink. In order to design an effective heat sink, some criterions such as thermal resistance, a low pressure drop and a simple structure should be considered.
In this work, a thermal design and evaluation method for heat sink is presented. The thermal hydraulic performances of the proposed heat sink are examined numerically using the finite differences method. In order to obtain generalized performance indicators that can be used to analyze plate-fin heat sink performances.

2. Literature review

When the literature is surveyed, a number of scholars have examined the air jet impingement on heat sink geometry. Hilbert et al. [3] reported a novel laminar flow heat sink with two sets of triangular or trapezoidal shaped fins on two inclined faces or a base. This design is efficient because the downward flow increases the air speed near the base of the fins where their temperatures are the highest. By having the cool air enter at the center of the heat sink and exit at the sides, the length of the fins in the flow direction is reduced so that heat transfer coefficient is increased. Jang and Kim [4] conducted an experimental study of a plate fin heat sink subject to an impinging air jet. The geometry of a heat sink in impingement flow is similar to that shown in Fig. 1. In this flow arrangement the air enters at the top and exits by the sides. Based on experimental results, a correlation for pressure drop and a correlation for its thermal resistance are suggested. They showed that cooling performance of an optimized microchannel heat sink subject to an impinging jet is enhanced by about 21% compared to that of the optimized microchannel heat sink with a parallel flow.

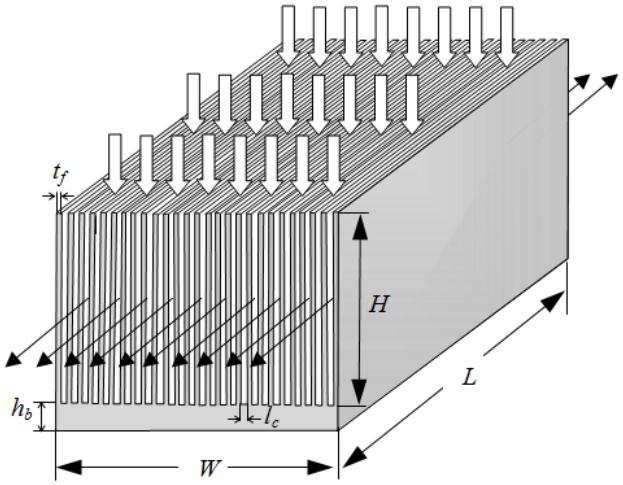

Fig. 1 Schematic diagram showing the physical model

Kang and Holahan [5] developed a one-dimensional thermal resistance model of impingement air cooled plate fin heat sinks to understand how the heat sink performance depends on different geometry variables. This simple model provides only an order of magnitude estimate of the thermal resistance. At a given pumping power, increasing the number of inlet/outlet channels requires an increase in the volume flow rate, but permits higher flow velocity, provides lower thermal resistance. Holahan et al. [6] modeled the impingement flow field in the channel between the fins as a Hele-Shaw flow. Conduction within the fin is modeled by superposition of a kernel function derived from the method of images. Convective heat transfer coefficients are adapted from existing parallel plate

correlations. Copland [7] performed theoretical, experimental, and numerical analyses on a manifold microchannel heat sink with multiple top inlets alternated with top outlets. Duan and Muzychka [8] performed the experimental investigation of the thermal performance with four heat sinks of various impingement inlet widths, fin spacing, fin heights and airflow velocities.

They developed a heat transfer model to predict thermal performance of impingement air cooled plate fin heat sinks for design purposes. Sathe and Sammakia [9] have presented a study of a new and unique high-performance air-cooled impingement heat sink.

The comparisons between numerical simulations an experimental data of the heat sink performance have been conducted. The effects of the fin thickness, inter-fin gap, nozzle width, and fin shape on heat transfer and pressure drop have been studied. The study showed that the pressure drop can be decreased by cutting the fins in the central impingement zone without sacrificing heat transfer rates. Shah et al. [10] demonstrated the results of a numerical analysis of the performance of an impingement heat sink designed for use with a specific blower as a single unit. The effects of the shape of heat sink fins, particularly near the center of the heat sink were examined. It is found that removal of fin material from the central region of the heat sink enhances thermal as well as the hydraulic performance of the sink. Shah et al. [11] studied extends of the previous work by investigating the effect of removal of a fin material from the end fins, the total number of fins, and the reduction in size of the hub fan. The reduction in size of the hub of the fan is found to be a more uniform distribution of air inside the heat sink, particularly near the center of the module.

In general, there are many testing processes for heat sinks which must be introduced in an effort to obtain the thermal and hydraulic performance of heat sinks.

If we take advantage of the numerical simulation to obtain some probable optimal design parameters before running experiments, the cost and research time can be reduced. In this paper, the numerical simulation of plate-fin heat sinks with confined impingement cooling in thermal-fluid characteristics will be investigated. The objective of this study is focused on the impingement flow plate fin geometry. The research objectives are to develop a simple model for predicting thermal and hydraulic performances of plate fin heat sink for impingement air cooling.

3. Physical and mathematical model

3.1. Physical model

Physical model of this study is illustrated in Fig. 1. In the configuration shown above, a heat sink with rectangular minichannels with hydraulic diameter D_h = 0.0029 m is heated from the bottom with the power (Q) generated by the CPU, which is absorbed by the sink and released to the atmosphere through the fins topped by an axial fan that blows air in impingement flow to dissipate heat in the atmosphere with a constant flow rate $\dot{V}$ (m^3/s).

The sink is made of aluminium of λ =237 W/m K. The power dissipation from the P4 CPU is set to 80 W [12]. The following assumptions are made to model heat transfer and fluid flow in the heat sink (2D fluid flow and 3D heat transfer) [13]: (1) steady state, (2) incompressible fluid, (3) laminar flow, because of the small fin spacing and low air flow rates, (4) constant fluid and solid properties, (5) negligible viscous dissipation, (6) negligible radiation heat transfer.

The dimensions of the heat sink considered in this work are listed in Table 1. Only a quarter of the heat sink was included in the computational domain, in view of the symmetry conditions.

Table 1
Geometry of the heat sink used in the computation

H, mm	h_b, mm	L, mm	l_c, mm	N_f	t_f, mm	W, mm
36	4	82	1.5	27	1	66

3.2. Mathematical model

The governing equations of continuity, momentum and energy are solved numerically using finite-difference scheme with boundary conditions as follows. The velocity is zero on all wall boundaries, and as flow is assumed to be hydrodynamically developed [14].

(1) Continuity equation

$$\nabla \vec{V} = 0 \tag{1}$$

(2) Momentum equation

- *for the fluid flow*

$$\rho\left(\vec{V}\,\nabla\right)\vec{V} = -\nabla p + \mu\nabla^2\vec{V} \tag{2}$$

- *for the solid*

$$\vec{V} = \vec{0} \tag{3}$$

(3) Energy equation

- *for the fluid*

$$\rho c_p\left(\vec{V}\,\nabla T\right) = \lambda_f\,\nabla^2 T \tag{4}$$

- *for the solid*

$$\lambda_s\nabla^2 T = 0 \tag{5}$$

The assumption of constant physical properties for the solid and the air allows decoupling the hydrodynamic equations of heat equations. Thus, solving the energy equation may be conducted after the convergence of computing hydrodynamics. In addition, the energy equation is linear; it converges faster than the Navier-Stokes. The equations were solved using a C++ developed code. The developed code is based upon the finite differences approach. The discretized equations are solved iteratively using the Gauss-Seidel method. Harmonic means are used to resolve differences between materials of different properties.

The Reynolds number of the impingement jet is

defined as

$$Re = \frac{|V_0| D_h}{\nu} \tag{6}$$

where $D_h = \frac{4A}{P_m} = \frac{4 h_a l_c}{2h_a + l_c}$ (7)

The average convection heat transfer coefficient h is calculated by

$$h = \frac{Q}{A_h (T_s - T_a)} \tag{8}$$

The average Nusselt number Nu is calculated by

$$Nu = \frac{h D_h}{k_a} \tag{9}$$

For very small distances from the rectangular duct inlet, the effect of curvature on the boundary layer development is negligible. Thus, it should approach the classical isothermal flat plate solution for developing flow in the entrance region of rectangular ducts ($L^* \to 0$) [14]

$$L^* = (L/2)/(D_h Re Pr) \tag{10}$$

$$Nu = 0.664 Re^{1/2} Pr^{1/3} \tag{11}$$

with $Pr = 0.707$ for the fluid (air).

Thermal resistance of the heat sink is calculated by

$$R_{th} = \frac{T_{\max} - T_\infty}{Q} \tag{12}$$

Note that boundary conditions of this problem are stated as shown in Figs. 2. and 3.

This enables to set properties in the solid and the fluid regions appropriately and solve the conjugate conduction convection problem [15].

The iterations were terminated when the residuals for the continuity, momentum equations were 1% of the characteristic flow rate and were 0.1% for the energy.

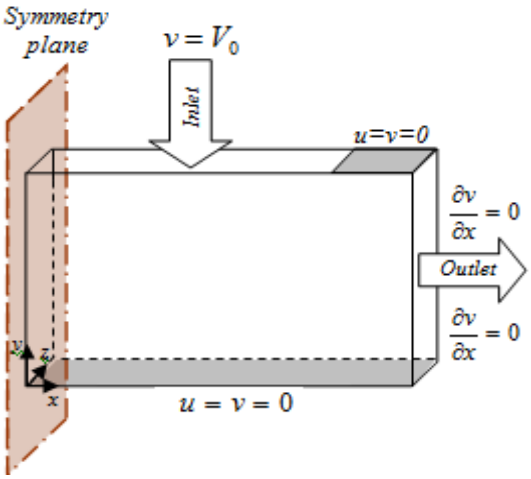

Fig. 2 Hydrodynamics boundary conditions

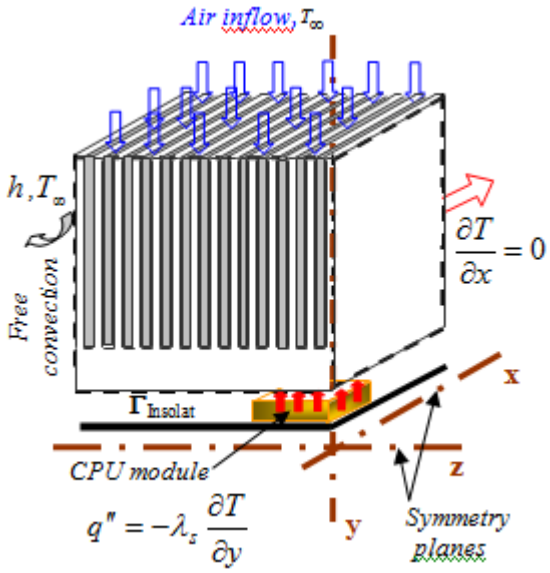

Fig. 3 Thermal boundary conditions

4. Results and discussion

The model is validated with the numerical results taken on the studied heat sink with the operating parameters listed in Table 2.

Table2

Operating parameters of the model

Parameter	Value	Description
V_0, m/s	5	inlet velocity
h, W/m² K	10	natural convection heat transfer coefficient (both sides of heat sink)
T_∞, °C	27	ambiante temperature
Q, W	80	power of heat source
A_{Die}, mm²	14×16	die surface of CPU
A_{CPU}, mm²	31×31	surface of CPU

Fig. 4 shows the distribution of static pressure through the channel of the heat sink (XY plane). The static pressure increases gradually up to the stagnation zone at the center where the velocity is the lowest then decreases in the direction of the air outlet. A low pressure drop is located at the exit channel where velocity is the highest.

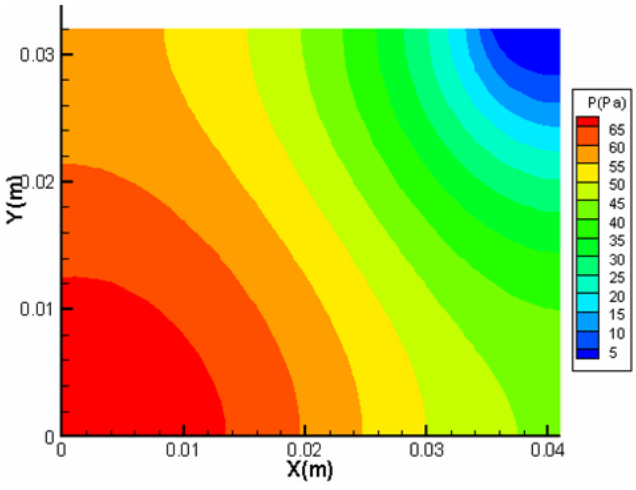

Fig. 4 Static pressure contours through the channel

The numerical results (Figs. 4 and 5) turn out that the pressure drops lie in the range of 5-62 Pa which is not so large. This is an advantage that improves heat transfer with less energy pumping.

Fig. 6 shows the average velocity field in the channel of heat sink. The results show clearly that the velocity slows down by going to the base until a breakpoint in the center. This velocity is increasing rapidly in the direction of the exit channel and reaches higher values than those at the entrance. This is the boundary layer phenomenon.

From Fig. 7, it is seen that the heat dissipation may be enhanced by increasing the cooling velocity.

The results of the temperature profile, Figs. 8, 9 and 10 show a peak (T_{max}) at the heat source, which is obvious but also high temperature gradient in the center of the sink where it should be a low airflow following. The temperature gradient source-air is about 19°C, so the thermal resistance R_{th} is calculated from Eq. (10) based on numerical results, it's of 0.2375°C/W.

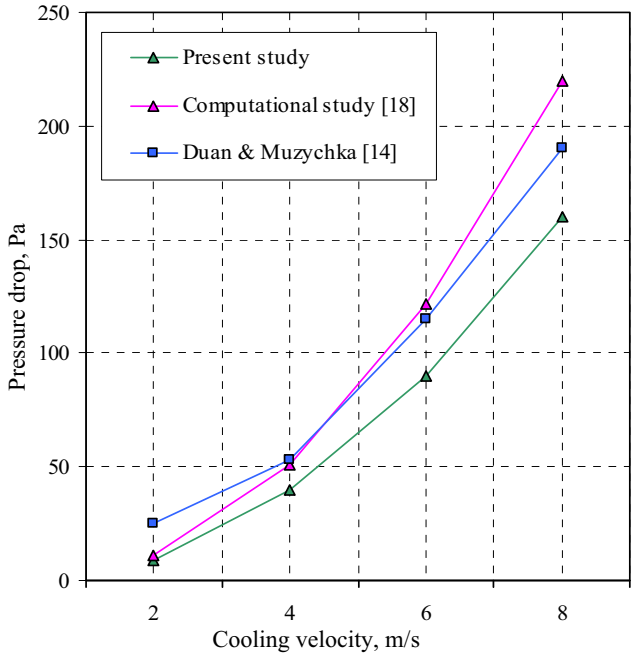

Fig. 5 Pressure drop through the minichannel as a function of cooling velocity (V_0)

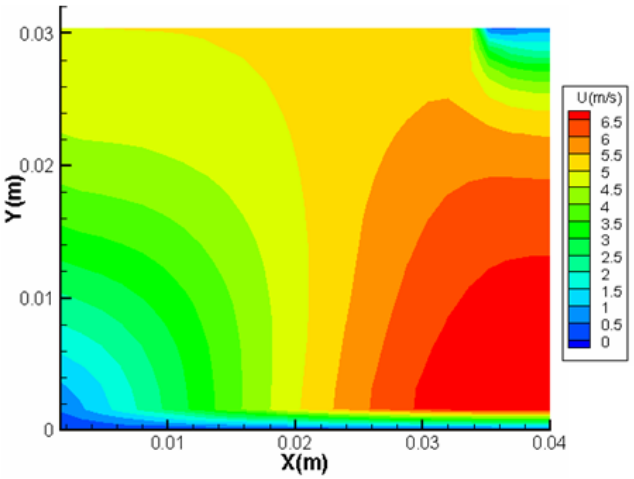

Fig. 6 Velocity contours through the channel

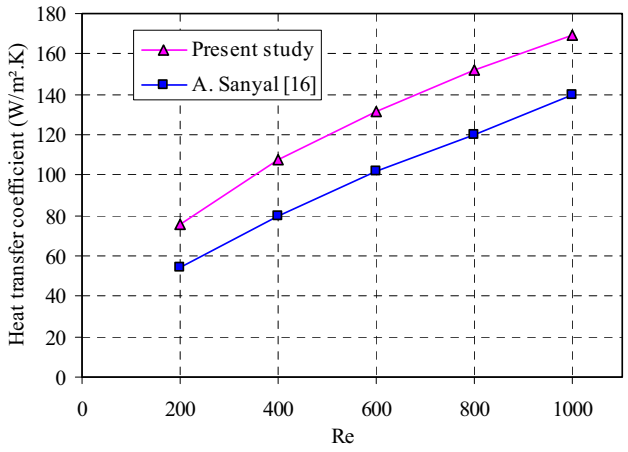

Fig. 7 Variation of convective heat coefficient as a function of cooling velocity (V_0)

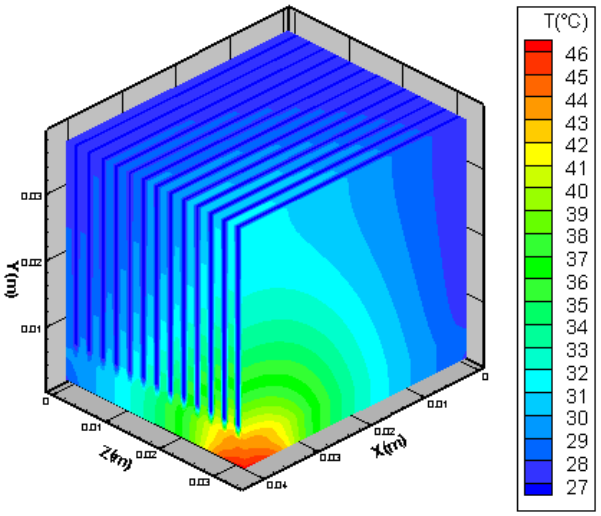

Fig. 8 Temperature distribution through the heat sink (3D)

Fig. 10 depicts the contours of temperature in the sink at the central cross-section. The maximum temperature is always observed in the heat source, this temperature under the mentioned conditions is about 46°C which is less than the temperature restricted by manufacturer.

Temperature distribution through the base of the sink is presented in Fig. 9, the results are obtained by the developed code. The hottest spot (T_{max} = 46°C) is located in the center of the base of the sink.

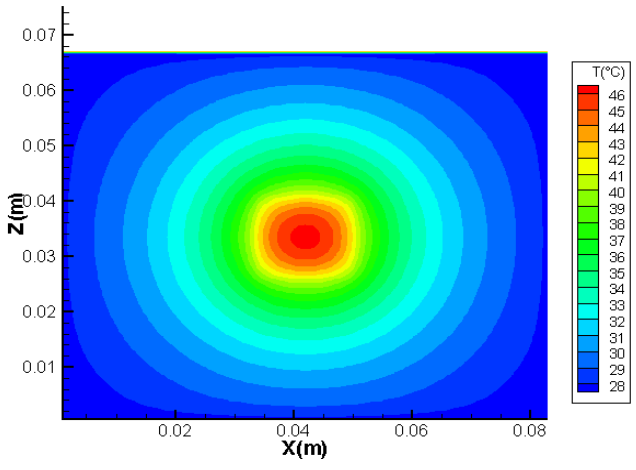

Fig. 9 Contours of temperature distribution on the base of the heat sink

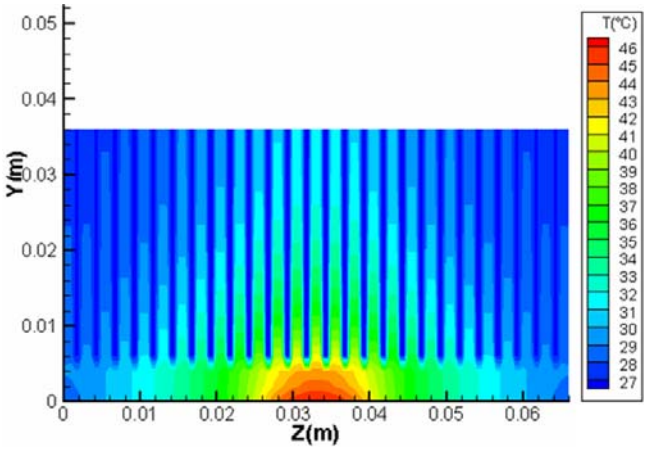

Fig. 10 Temperature distribution in the sink at the central cross-section

This is due primarily to the presence of heat source at this level and then because the fluid cooler has the lowest traffic there (stagnation zone).

In addition, heat is dissipated in both longitudinal and transverse directions, where it appears that the length of the fin beyond a limit of 38 mm does not contribute to temperature decrease and so can be reduced. But, according to the width, temperature can be dissipated by further wide.

5. Conclusion

In this research work, thermal and hydraulic characterizations have been carried out on a parallel plate heat sink considering real operating parameters using the developed code. The results show that impingement air flow on minichannel heat sink appears to have advantages for heat transfer. The thermal and hydrodynamic performances computed by the developed code show that the chip delivers up to 80 W it is adequately cooled by the studied heat sink as recommended by the Intel manufacturer. The effect of Reynolds number on the convective heat transfer coefficient is examined. The results also show that there is potential for optimizing the geometric design. This study will benefit the designers involved in electronic cooling. It can be used to select or design heat sink for effective thermal management in electronic assemblies. The results obtained in numerical experiments have been compared with the literature results and found to be in a good agreement.

References

1. **Yue-Tzu Yang; Huan-Sen Peng**. 2008. Numerical study of pin-fin heat sink with un-uniform fin height design, Int. J. of Heat and Mass Transfer 51: 4788-4796.
2. **Nishino, K.; Samada, M.; Kasuya, K.; Torii, K.** 1996. Turbulence statistics in the stagnation region of an axisymmetric impingement jet flow, Int. J. Heat fluid flow 17: 193-201.
3. **Hilbert, C.; Sommerfeldt, S.; Gupta, O. and Herrell, D.J.** 1990. High performance micro-channel air cooling. Proc. 6th IEEE Semiconductor Thermal and Temperature Measurement Symposium, Scottsdale, Arizona: 108-113.
4. **Jang, S.P. and Kim, S.J.** 2005. Fluid flow and thermal characteristics of a Microchannel heat sink subject to an impinging air jet, J. of Heat Transf. 127: 771-777.
5. **Kang, S.S. and Holahan, M.F.** 1995. Impingement heat sinks for air cooled high power electronic modules. Proc. ASME HTD, vol. 303, National Heat Transfer Conference, Portland, OR, Vol. 1: 139-146.
6. **Holahan, M.F.; Kang, S.S. and Bar Cohen, A.** 1996. A flowstream based analytical model for design of parallel plate heat sinks. Proc. ASME HTD, vol.339, National Heat Transfer Conference, vol. 7: 63-71.
7. **Copland, D.** 2000. Optimization of parallel plate heat sinks for forced convection. Proc. Sixteenth Semi Therm Symposium: 266-272.
8. **Duan, Z.P, Muzychka, Y.S.** 2004. Impingement air cooled plate fin heat sinks Part I- Pressure drop model. 2004 IEEE, Inter Soc. Conf. on Therm. Phenom.: 429-435.
9. **Sathe, S.B.; Sammakia, B.G.; Wong, A.C. and Mahaney, H.V.** 1995. Anumerical study of high performance air cooled impingement heat sink. Proc. ASME HTD, vol. 303. National Heat Transfer Conference, Portland, OR, vol. 1: 43-54.
10. **Shah, A.; Sammakia, B.G.; Srihari, K.; Ramakrishna, K.** 2004. A numerical study of the thermal performance of an impingement heat sink fin shape optimisation, IEEE Trans. Compon. Packag. Technol. 27(4): 710-717.
11. **Shah, A.; Sammakia, B.G.; Srihari K.; Ramakrishna, K.** 2006. Optimization study for a parallel plate fin impingement heat sink, J. Electron. Packag 128: 311-318.
12. **Intel®** Pentium® 4 Processor on 90 nm Process Thermal and Mechanical Design Guidelines. Design Guide, 2004.
13. **Lee, P.S.; Garimella, S.V.** 2006. Thermally developing flow and heat transfer in rectangular microchannels of different aspect ratios, International Journal of Heat and Mass Transfer 49: 3060-3067.
14. **Duan, Z.P.; Muzychka, Y.S.** 2006. Experimental investigation of heat transfer in impingement air cooled plate fin heat sinks, J. of Electronic Packaging 128: 412-418.
15. **Pantakar, S.V.** 1980. Numerical Heat Transfer and Fluid Flow. Hemisphere. Washington. 195p.
16. **Sanyal, A.** 2006. Numerical Study of heat transfer from Pin Fin heat Sink using steady and pulsated impinging jets. Master of Science Thesis. Indian Institute of Science. 81p.
17. **Beriache, M.; Mokhtar Saïdia, L.; Bettahar, A.** 2010. Numerical characterization of hydraulic and thermally performance of a minichannels heat sink subjected to impingement air flow. Annual Congress of Thermal Sciences, French Society of Thermal Sciences, vol.1: 163-169.
18. **Mokhtar Saïdia, L.** 2009. Numerical computation of forced convection in duct with array of heated plates. Master of Science Thesis. University of Chlef, Algeria. 104p.
19. **Holman, J.P.** 1996. Heat transfer McGraw-Hill Book Company, New York, SI Metric Edition**.** 696p.
20. **Builder C++** User's Guide. Borland Software Corporation, 2002.

M. Beriache, A. Bettahar, L. Loukarfi,
L. Mokhtar Saidia, H. Naji

MAŽAKANALIO ORO SROVĖS AUŠINTUVO HIDRAULINIŲ IR ŠILUMINIŲ CHARAKTERISTIKŲ SKAITINIS TYRIMAS

R e z i u m ė

Smūginis oro aušinimas priverstine konvekcija pritaikytas šilumai išsklaidyti didelės galios elektroniniuose įtaisuose su lygiagrečiais radiatoriniais aušintuvais. Aptariami oro srovės greičio kanaluose su padidintais paviršiais komponentai. Slėgio kritimas ir šiluminės charakteristikos analizuojamos naudojant patobulintą skaitinį C++ kodą. Nagrinėjamas šiluminės ir hidraulinės charakteristikos priverstinio konvekcinio aušinimo oru sąlygomis. Išanalizuoti ir grafiškai parodyti hidrauliniai parametrai, įskaitant greičio pobūdį, statinio slėgio pasiskirstymą ir slėgio kritimą aušinimo metu. Be to, yra išnagrinėtos aušinimui naudojamo aliuminio šiluminės charakteristikos, įvertinant erdvinį temperatūros pasiskirstymą radiatoriuose ir aušintuve. Kaip ir tikėtasi, siūlomo modelio duomenys, nustatyti skaitiniu būdu, gerai sutampa su gautais ankstesniuose tyrimuose.

M. Beriache, A. Bettahar, L. Loukarfi,
L. Mokhtar Saïdia, H. Naji

NUMERICAL STUDY ON HYDRAULIC AND THERMAL CHARACTERISTICS OF A MINICHANNEL HEAT SINK WITH IMPINGING AIR FLOW

S u m m a r y

In this study impingement air cooling mode of forced convection is adopted for heat dissipation from high power electronic devices in associated with a parallel fin heat sink. Components of airflow velocity in the channel of the extended surfaces are discussed. Pressure drop and other thermal performances are analyzed numerically by a C++ developed code. Thermal and hydraulic characterization of heat sink under cooling condition of air-forced convection is studied. The hydraulic parameters including velocity profiles, distribution of static pressure and pressure drop through the heat sink are analyzed and presented schematically. Furthermore, the thermal characteristic of the aluminum approach of cooling is studied by utilizing the contours of the three dimensional temperature distributions through the fins, base heat sink and the heat sink body. The performance of the proposed model computed by the numerical calculation is high compared to current heat sinks as expected of the previous studies.

М. Бериацхе, А. Беттахар, Л. Лоукарфи,
Л. Мокхтар Саидиа, Х. Наюи

ЧИСЛЕННОЕ ИССЛЕДОВАНИЕ ГИДРАВЛИЧЕСКИХ И ТЕПЛОВЫХ ХАРАКТЕРИСТИК МИНИКАНАЛЬНОГО ОХЛАДИТЕЛЯ ПОТОКА ВОЗДУХА

Р е з ю м е

В данном исследовании ударный тип охлаждения воздухом с принудительной конвекцией применен для рассеивания тепла в электронных устройствах высокой мощности при охлаждении параллельными радиаторами. Обсуждаются компоненты скорости потока воздуха в каналах с увеличенными поверхностями. Падение давления и тепловые характеристики анализируются с использованием модернизированного числового кода C++. Исследуются тепловые и гидравлические условия принудительного конвекционного охлаждения потоком воздуха. Рассмотрены и показаны графически гидравлические параметры, учитывая характеристику скорости, распределение статического давления и его снижение в процессе охлаждения. Кроме того, рассмотрены тепловые характеристики алюминия при применении его для охлаждения с учетом пространственного распределения температуры в радиаторах и конструкции охладителя. Определенные числовым методом данные предлагаемой модели хорошо соответствуют, как и предполагалось, с результатами, полученными в более ранних исследованиях.

Received September 28, 2010
Accepted March 15, 2011